DUCTILE FRACTURE MECHANISMS IN AN AUSTENITIC STAINLESS STEEL

I. J. O'Donnell, B. L. Eyre and F. W. Noble

Department of Metallurgy and Materials Science, University of Liverpool, England

ABSTRACT

In this study the relationships between microstructure, impurity solute leve ductility and fracture toughness have been investigated on casts of austenit 316 stainless steel in different heat treated conditions, using optical and electron microscopy.

KEYWORDS

Microstructure; stress state; void nucleation, growth and coalescence; ductility; fracture toughness.

INTRODUCTION

A continuing unresolved problem in the study of ductile fracture in steels i the relationship between metallurgical factors such as microstructure, solut levels and distribution and the micro-mechanisms governing fracture toughnes Although there is a large body of information on ferritic steels, comparitiv ly few results have been obtained on austenitic steels and, in particular, from 316 stainless steel.

Type 316 stainless steel is widely used in power generation and chemical pla operating at elevated temperatures. The steel is normally introduced into service in the solution treated condition, but prolonged heating at elevated temperatures results in the precipitation of carbides and intermetallic phas It is also likely that there is a simultaneous redistribution of tramp eleme and other solutes. The results reported in this paper are from an extensive study of the effect of these metallurgical changes on the room temperature ductile fracture characteristics of 316.

EXPERIMENTAL PROCEDURE

Materials and Heat Treatment

The experiments were performed mainly on two special casts of type 316 stainless steel: a high purity cast, SC1, and a 'doped' cast, SC2, identical to SC1 except for an increased phosphorus level. The compositions of these casts are given in Table 1.

The two alloys were studied in the heat treated conditions detailed below:

Condition A: Solution treated (ST) for 3h at 1050°C followed by an air cool;

Condition B: Solution treated and aged for 500h at 800°C.

The microstructure of the steels in both conditions was characterised using optical and electron microscopy to establish the inclusion content and distribution and, in the aged material, the precipitate distribution and morphology. The types of inclusions and precipitates present were determined using EDX analysis on carbon extraction replicas using a Philips 400T microscope in STEM mode.

TABLE 1 Cast Analyses

	SC1	SC2
C%	0.08	0.07
Si%	0.52	0.52
Mn%	1.91	1.94
P%	0.001	0.024
Cr%	17.19	17.32
Fe%	BAL	BAL
Mo%	2.57	2.59
N PPm	548	523
Ni%	11.99	12.08
Sn PPm	-	-

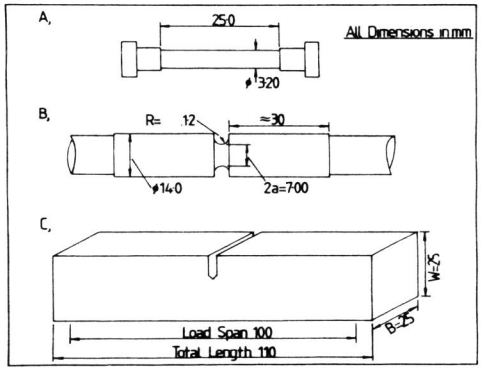

Fig. 1. Tensile specimen geometries.

Mechanical Testing

Room temperature tensile tests were performed on both plain and notched tensile specimens using a servo-mechanical Instron 1185 testing machine. The specimen geometries are shown in Fig. 1. The notched samples introduce a hydrostatic component into the stress distribution in the material, quantified by the ratio of the mean stress, σ_m, to the effective stress, $\bar{\sigma}$. The value of this ratio for the notch geometry employed is 1.23 compared with 0.33 for a plain specimen. Strains in the notched specimens were determined using lateral extensometry and the post-UTS strains in the neck of the plain specimens were also evaluated in terms of a reduction in diameter. Several tests on both types of specimen were interrupted at various different strains to allow the specimens to be sectioned for metallographic examination of the deformed material.

Fracture toughness measurements were made using fatigue pre-cracked, three-point bend specimens. Crack tip opening displacements, σ, and crack depths, Δa, were measured optically on sections cut from the deformed specimens and the results were plotted in the form of an R-curve of δ vs crack advance,

enabling the critical C.T.O.D. value, δ_i, to be determined by extrapolation

For reasons of material availability, these tests were performed on materia of different origins to SC1 and SC2, but of nominally the same specificati

Metallography and Fractography

Void nucleation and growth observations were made on longitudinally section tensile specimens strained into both the plastically stable and unstable regimes before the tensile test was stopped. The sections were carefully p pared using techniques designed to minimise the possibility of smearing su face material into voids exposed in the sections, and were examined using optical and electron microscopy, and in the aged material thin foils were p pared from the sections for observation in the T.E.M. Fractographic obser ations were made using S.E.M. and optical microscopy.

RESULTS

Microstructure

Both materials exhibited identical microstructures in the solution treated condition, consisting of a random distribution of equi-axed inclusions in a austenitic matrix, as illustrated for SC2 in Fig. 2. The volume fractions inclusions was found to be 0.09%, of which about 89.5% were of the Cr-gala type (Kiessling, 1964) 7.5% chromite and 3% other types (Al_2O_3 and SiO_2).

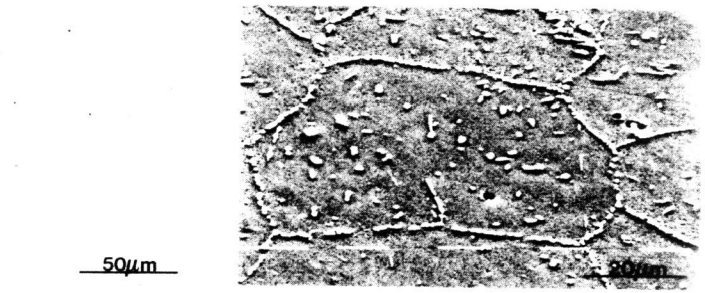

Fig. 2. SC2 Solution treated.

Fig. 3. SC1 Aged for 500hr at 800° (SEM)

the aged material, precipitation of second phases occurred both on the grain boundaries and in the matrix. Again, there was no difference between the t materials and an example of the microstructure of aged SC1 is shown in Fig. The population of precipitates in this material was found to consist of 58% $M_{23}C_6$, 29.3% Chi phase, 10.3% Laves' phase and 2.3% sigma phase particles.

Mechanical Properties

Tensile test data for plain tensile specimens is given in Table 2a. The

results show that, within the scatter, strength and ductility levels are comparatively insensitive to material composition, but there is an effect of heat treatment on ductility, the aged material showing a significantly reduced strain to failure. The data in Table 2a shows that the pre-UTS strain is comparatively unaffected and that most of the reduction in strain to fracture is in the post-UTS component.

TABLE 2a Tensile Data for the Plain Specimens.

	0.2% P.S. N/mm^2	Pre-UTS	Post-UTS	Total Strain
SC1 ST	239.5	0.40	1.45	1.85
SC2 ST	243.8	0.49	1.15	1.64
SC1 Aged	222.3	0.42	0.49	0.91
SC2 Aged	233.6	0.39	0.45	0.84

TABLE 2b Tensile data for the Notched Specimens

	Pre-UTS	Post-UTS	Total Strain
SC1 ST	0.42	0.46	0.88
SC2 ST	0.43	0.56	0.99
SC1 Aged	0.25	0.06	0.31
SC2 Aged	0.32	0.02	0.34

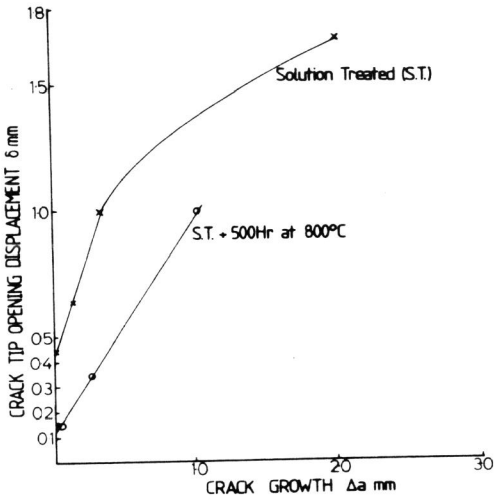

Fig. 4. Fracture toughness R-curve.

The results for the notched specimens are given in Table 2b and it can be seen that the behaviour is broadly similar, but the decrease in post-UTS strain to fracture resulting from the ageing treatment is more emphatic. For both materials and conditions the presence of the notch has resulted in a decrease in ductility relative to the plain specimens, but, again, there is no detectable effect of composition on the mechanical properties.

The decrease in strain to failure revealed by the tensile data is reflected in the fracture toughness results plotted in Fig. 4. These R-curves show that the fracture toughness of the aged material (measured by δ_1) is reduced by a factor of 4, compared with solution treated material.

Metallography and Fractography

Figures 5 and 6 show S.E.M. fractographs of plain and notched specimens respectively of SC2 material in the solution treated condition. In both cases fracture has occurred by the coalescence of inclusion nucleated voids. The major difference between the plain and notched cases is in the shape of the larger voids, with the depth to diameter ratios being 1-2 in the notched specimens and 3-5 in the plain specimens. Corresponding fracture surfaces for the aged material are shown in Figs. 7 and 8. In this material the voids are on a

much finer scale and can be identified with nucleation occurring at both the inter- and intra-granular precipitate particles. Although the fracture surfaces still show largely transgranular fracture, the tendency for cracking to follow the grain boundaries is apparent in the development of intergranular cracks at right angles to the fracture surface, parallel to the tensile axis.

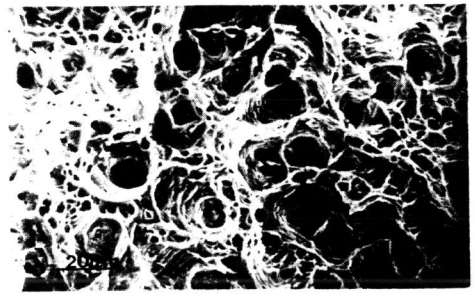

Fig. 5. Fractograph of a SC2 ST plain tensile specimen.

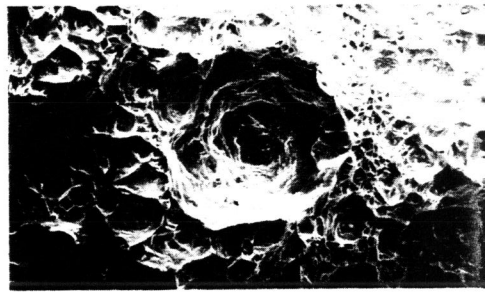

Fig. 6. Fractograph of a SC2 ST notched tensile specimen.

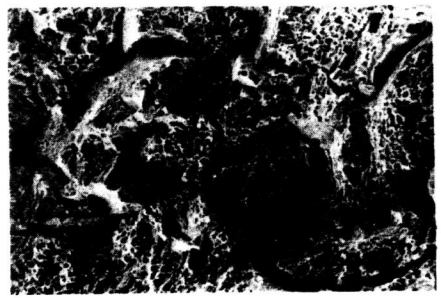

Fig. 7. Fractograph of a SC2 aged plain tensile specimen.

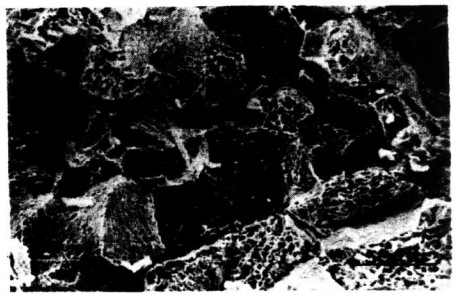

Fig. 8. Fractograph of a SC2 aged notched tensile specimen.

The general features of the fractures revealed by the fractography were confirmed by the longitudinal sections. Figures 9 and 10 show the pattern of void coalescence and crack formation in the solution treated material, while Figs. 11 and 12 show the same process, involving precipitate nucleated voids in the aged material. The tendency for grain boundary void formation and subsequent cracking is clearly visible in Figs. 11 and 12, as are the intergranular secondary cracks forming parallel to the tensile axis.

Optical microscopy on deformed S.T. material revealed little evidence of void nucleation prior to the U.T.S. ($\varepsilon \sim 0.5$) and at the U.T.S. about 10% of the inclusions were observed to have nucleated voids, this percentage increasing rapidly with non-uniform, post U.T.S. strain. Lateral growth of these voids was first detectable after a strain of some 0.75. Void formation in the aged material at precipitate particles was more amenable to study by T.E.M. and this technique enabled voids to be detected at strains as low as 15%, while foils prepared from plain tensile specimens with only 5% strain showed no

evidence of any voids or precipitate cracking.

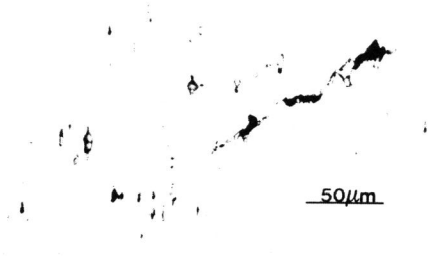

Fig. 9. Void coalescence from inclusion nucleated voids in a SC2 ST plain tensile specimen

Fig. 10. Formation of the central crack in a SC2 ST plain tensile specimen.

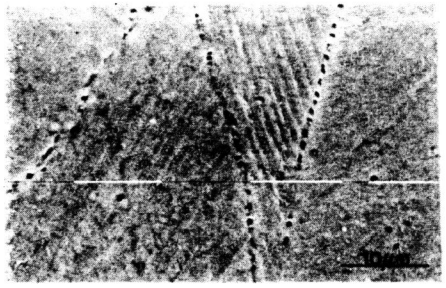

Fig. 11. Void growth from precipitate nucleated voids in a SC2 aged plain tensile specimen.

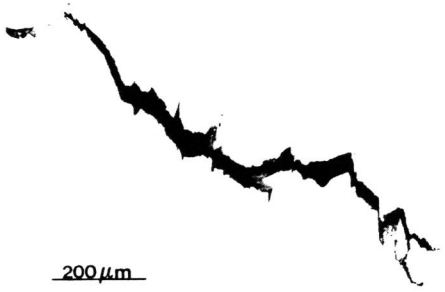

Fig. 12. Formation of the central crack in a SC2 aged plain tensile specimen.

DISCUSSION

The observation that the inclusion nucleated voids in 316 are only detectable after a considerable amount of deformation contrasts with the behaviour of ferritic steels in which such voids are observed to develop much earlier in the deformation process, soon after yield (Gladman, 1979). The inclusions in ferritic steels are usually elongated, deformable sulphides and are larger, in general, than the spherical, undeformable oxide inclusions encountered in 316. Although a size effect on void nucleation is to be expected (Cox and Low, 1974), it seems more probable that the delayed nucleation of voids in 316 reflects a stronger inclusion-matrix interface in this material compared with the weak interface characteristic of the sulphide inclusions in a ferritic matrix.

It has been suggested that void formation by interfacial decohesion will be

controlled by the attainment of a critical stress at the interface (Argon, and Safoglu, 1975; Beremin, 1981) derived from a combination of local stres associated with strain inhomogeneities and the direct effect of applied ten sile stress. The former contribution is expected to be dependent on the ov all strain in the sample and at a given stress level a larger void density to be expected in specimens deformed to higher strains. This was found to the case when a comparison was made between a deformed notched specimen and plain specimen deformed to such an extent that strain hardening raised the level of applied stress to that encountered by the notched specimen. Howeve when a similar comparison was made between notched and plain specimens de- formed to the same strain, the higher tensile stress encountered by the notched specimen was accompanied by a significantly higher void density, co firming the significance of direct stress in the nucleation process.

The extent to which void nucleation at carbides in the aged material depend on the attainment of a critical stress condition is less clear. The T.E.M. results appeared to show that carbide cracking rather than interfacial de- cohesion was the predominant mechanism of void formation at low strains, and this is in agreement with earlier work by Barnby (1967), who envisaged the cracking to result from a dislocation in pile-up mechanism, subsequently analysed by Smith (1966). This model would suggest that void nucleation by carbide cracking is not directly influenced by the direct stress and should occur at more or less the same strain in plain and notched specimens. The T.E.M. results, however, were not sufficiently conclusive as to allow this suggestion to be verified.

The fractography results and the observations on sectioned specimens indica that while the ductility of S.T. material is controlled by the interlinkage inclusion nucleated voids, that of aged material is dominated by the inter- linkage of carbide nucleated voids. Because of the very close spacing of t carbides along the grain boundaries, it is expected that the interlinkage pr cess would occur most rapidly along these boundaries and that the crack path would be predominantly intergranular. However, while the tendency towards intergranular fracture is clearly visible in Figs. 7 and 12, in the form of cracking along the grain boundaries lying parallel to the tensile axis, the main crack path is predominantly transgranular, particularly in the plain specimens, but slightly less so in the notched specimens. The reason for t apparently anomalous behaviour lies, we believe, in the appreciable deform- ation which necessarily precedes ductile fracture and this will be considere below.

In the S.T. plain specimens the true strain in the neck at fracture is of th order of 1.5, resulting in the grains in these regions being elongated to aspect ratios of the order of 5 or 6. Similarly, because void nucleation occurs comparatively early on in this strain history ($\varepsilon \sim 0.4$), then the voi too will be very elongated (lateral growth being small in comparison) and th fractographs of the fracture surface of the S.T. specimens confirm this. I the notched samples both these effects are less pronounced because of the reduced strains to fracture. A consequence of the 'fibrous' grain texture the heavily deformed material is that an intergranular fracture path necessi ates extensive crack growth parallel to the tensile axis in order that the comparitively short, isolated segments of boundary lying normal to the tensi axis can be linked. It is envisaged, therefore, that in the aged material, although the nucleation of a ductile crack on these transverse segments will occur fairly readily by void interlinkage, further propagation across the specimens will be blocked by the longitudinal boundaries until sufficient co alescence has occurred between the voids nucleated within the grains as to permit transgranular crack growth. The hoop stresses resulting from the nec

(or notch) geometry will serve to drive some intergranular crack segments along the boundaries lying parallel to the tensile axis (into areas of reduced stress), but the fracture surface normal to the tensile axis will be mainly transgranular in nature. It appears, therefore, that the deleterious effect of the closely spaced grain boundary precipitates in promoting easy void coalescence is to some extent offset by the difficulty experienced by an intergranular crack propagating through a heavily deformed, fibrous structure.

CONCLUSIONS

1. Ageing solution treated type 316 steel at 800°C results in the precipitation of carbides and intermetallic phases and this both reduces the ductility to fracture and fracture toughness.

2. In contrast, no evidence was found for phosphorus at the 240ppm level influencing the fracture processes in either the solution treated or aged specimens.

3. In the solution treated material void nucleation occurs by the decohesion of the inclusion matrix interface under the combined action of direct stress and local stress. The large inter-inclusion spacing necessitates substantial void growth prior to coalescence and the material in this condition is commensurately ductile and tough.

4. Void nucleation at carbides occurs at low strains and these voids dominate the fracture process as a result of the small spacing between the carbide particles - especially along the grain boundaries - giving a significant reduction in toughness and ductility, but with little effect on strength.

5. Although crack formation by void coalescence along the grain boundaries occurs readily in the aged material, the heavy deformation which precedes fracture leads to a grain structure inimical to the development of an intergranular fracture path.

ACKNOWLEDGMENTS

One of us (I.J. O'Donnell) is grateful to the S.E.R.C. for the award of a research studentship.

The research was made possible by a grant from the U.K.A.E.A. and we wish to thank Drs. A. Cowan and C. Picker for helpful discussion.

REFERENCES

Argon, A.S., J. Im and R. Safoglu (1975). Met. Trans., 6A, 825-837.
Barnby, J.T. (1967). Acta Met., 15, 903-909.
Beremin, F.M. (1981). Met. Trans., 12A, 723-731.
Cox, T.B., and J.R. Low (1974). Met. Trans., V5, 1457-1470.
Gladman, T. (1979). The effects of inclusions on mechanical properties. In F.B. Pickering (Ed.), Inclusions, The Institution of Metallurgists, Monograph No. 3, Chameleon Press, London. pp. 157-171.
Kiessling, R., and N. Lange (1964). Non-metallic inclusions in steel. Iron and Steel Institute, Special report 90.
Smith, E. (1966). In A.C. Stickland (Ed.), Yield and Fracture, Conf. Proc., Institute of Physics and Physical Society, London. pp.36-46.